



Spectroscopic and Electrical Properties of Sodium Alginate/TiO₂-Carbon Nanotube Composite



Naglaa A. Shahin and Reham K. Abd El Hamid*

Physics Department, Faculty of Women for Arts, Science and Education, Ain Shams University, Cairo, Egypt.

THIS work describes the preparation and characterization of Sodium Alginate (NaAlg) treated with Titanium dioxide (TiO₂)-Carbon nanotube(CNT). The morphology of composites was investigated by scanning electron microscope (SEM) showing the CNT coated with NaAlg and the TiO₂ dispersed in the NaAlg matrix. Fourier Transform Infrared Spectroscopy (FTIR) was applied for characterization of NaAlg composite with TiO₂/CNT, the whole alginate presented bands in the region of 948-780 cm⁻¹. The structure characteristics and surface properties of the samples were characterized by Electrical Conductivity that was measured in the range of (42 Hz-1 MHz). The study concluded that the introduction of TiO₂/CNT resulted in improvement in electrical conductivity of the NaALg matrix.

Keywords: Sodium alginate, Titanium dioxide, Carbon nanotube, FTIR, SEM, Electrical conductivity.

Introduction

The wide use of heavy metal solutions in many industrial activities such as battery manufacturing and painting results in the generation of large quantities of effluent that contains high level of heavy metals, most of which are toxic and carcinogenic. Therefore, their presence in the aquatic ecosystem poses the human health risks due to their non-degradable and persistent nature. The strict regulations concerning the presence of heavy metals in the aquatic environment have been introduced in recent years [1]. Consequently, the treatment of industrial effluents is a challenging topic in the environmental field and many conventional methods are used for the removal of toxic metals from aqueous solutions such as chemical precipitation, liquid-liquid extraction, ion-exchange adsorption [2], filtration [3], electrochemical treatment, reverse osmosis, membrane technologies, and evaporation recovery. Among these methods, adsorption may be a suitable wastewater technology competitive with the other conventional technologies to

remove heavy metals. Currently, research is focused on the use of bio adsorbents which are inexpensive, biodegradable, and available in large quantities to support potential demand [4]. CNT were first reported by Iijima in 1991 and they possess unique mechanical, optical, electrical and thermal conductivity along with thermal and chemical stability. Due to the unique properties of CNT, researches have focused on utilizing these remarkable characteristics for engineering applications such as polymeric composites, hydrogen storage, actuators, chemical sensors, and nano-electronic devices. CNT have high surface-to-volume ratio, and that is why they offer chemically facile sites that can be functionalized with additives thereby resulting in a strong interfacial bond with the matrix [5]. CNTs have been widely used as adsorbents to remove inorganic and organic contaminants from wastewater in recent years. The exceptional properties of CNTs such as high mechanical strength, large specific surface area, hollow and layered structures, and high chemical and thermal stabilities, make them a good candidate as adsorbent and allow the

*Corresponding autor e-mail: rehamebaad1974@hotmail.com

Received 28/2/2019; Accepted 19/6/2019

DOI: 10.21608/EJCHEM.2019.12908.1808

©2019 National Information and Documentation Center (NIDOC)

great promising applications in environmental protection [6]. However, widespread usage of CNTs will cause increased emissions to the aquatic environment and result risk of contact risk with CNTs [7]. Because of the poor degradability [8] and toxicity of CNTs, they should be removed from the drinking water as far as possible. As it is difficult to remove CNTs from water using conventional separation methods due to their nano-sized structures, this limitation may be the bottleneck to obstruct CNTs to be widely used as adsorbents in environmental protection in the future [9]. Titanium dioxide (TiO_2) is one of the most interesting photocatalysts due to its remarkable photocatalytic performance, easy availability, long-term stability, and nontoxicity [10]. When the light irradiation has energy larger than the band-gap energy of TiO_2 (3.20 eV for anatase and 3.03 eV for rutile), the photoexcitation of TiO_2 generates electron–hole pairs. These pairs initiate a cascade of events producing reactive oxygen species (ROS), which are involved in pollutants degradation on TiO_2 particles surface. However, some drawbacks arise when TiO_2 is applied as a photocatalyst: (1) the photo generated electron–hole pairs can recombine quickly, which affects the photocatalytic efficiency, and (2) TiO_2 can only be excited with ultraviolet (UV) light, which is less than 5% of sunlight, because of its wide band gap [11]. These disadvantages result in a low photocatalytic performance for environmental applications. Therefore, to efficiently apply abundant sunlight as a green process, a series of strategies, such as metal/nonmetal elements doping and coupling with other functional materials has been adopted to design visible-light-sensitive TiO_2 -based photocatalysts by introducing an extrinsic band gap with lower energy, suppressing electron–hole recombination rate and increasing the surface charge carrier transfer rate of TiO_2 [12-14]. The application of photocatalytic degradation for the decontamination of industrial wastewater and the remediation of ground or drinking water has become the focus of massively relevant research [15-17]. In the conventional process of wastewater treatment, TiO_2 nanoparticles are generally used as a slurry system due to the large surface area of the catalysts available for high photocatalytic efficiency [18]. However, the elimination of TiO_2 suspended in treated water causes running costs and induces secondary pollution, which greatly restricts its practical applications. Consequently, several methods have been utilized to immobilize

TiO_2 nanoparticles on various substrates, such as glass stainless steel plates [19] CNTs and polymers [20]. Alginate, a natural polysaccharide extracted from brown seaweeds, is a very promising bio adsorbent. It is preferred over other materials because of its various advantages such as biodegradability, hydrophilic properties, non-toxicity, natural origin, abundance, and presence of binding sites due to its carboxylate functions [21]. The carboxylate groups of the polymer provide the ability to form biodegradable gels in the presence of multivalent cations and more specifically with calcium ions via ionic interactions. In the environmental field, alginate beads are widely used for the removal of heavy metals from wastewater. In addition, alginate beads containing different components to enhance the adsorption capacity of the system are also widely investigated [22].

Materials and Method

Films with different weight percentage of NaAlg substituted with CNT/ TiO_2 are prepared using solution casting technique. NaAlg was dissolved in distilled water and stirred with magnetic stirrer at ambient temperature until it is completely dissolved. CNT/ TiO_2 was added to the previous solution of NaAlg at a ratio of 2.5:97.5 wt.%, 5:95 wt.% and 10:90 wt.% and stirred until there were no phase changes. The mixtures were then cast into glass Petri dishes and left to dry in air.

Results and Discussion

FTIR Analysis

The FTIR spectrum of NaALg 100%, NaAlg 97.5%/(CNT/ TiO_2)2.5%, NaAlg 95%/(CNT/ TiO_2)5%, and NaAlg 90%/(CNT/ TiO_2) 10% composites are shown in Fig. (1:a,b,c,d) Sodium alginate (1:a) presented a band centered at 3343 cm^{-1} corresponding to the functional group O-H. The band at 2945 cm^{-1} is attributed to the stretching vibration of C-H. The band observed at 2166 cm^{-1} is attributed to the group CO_2 group. The increase in the band intensity at 1603 cm^{-1} is corresponding to the carboxyl group band. Bands observed at 1417 cm^{-1} and 1358 cm^{-1} are attributed to the asymmetrical stretching of the COO^- and C-O groups. Bands at 1101 cm^{-1} and 1034 cm^{-1} are associated with the stretching vibrations corresponding to the C-O group. Besides, bands at 920 cm^{-1} and 822 cm^{-1} are attributed to the C-H vibration of the pyranose (ring of the alginate) group [23]. Compared with the spectrum of NaAlg

beads and NaAlg treated with CNT/TiO₂ (1:b,c,d), the strong band of NaAlg beads at 1603 cm⁻¹ which assigned to the carboxyl group shifted from 1608 cm⁻¹ to 1627 cm⁻¹ respectively indicating the specified intermolecular hydrogen bonds between the carboxyl group of NaAlg and CNT/TiO₂ [24]. The band at around 1704 cm⁻¹ corresponding to the stretching mode of the carboxylic acid groups of the CNT [25], which is observed at the concentration of 10% of CNT/TiO₂. The spectrum shows that the prominent band around 600 cm⁻¹ is due to stretching vibration of Ti-O-Ti nanoparticles [26]. The adsorption band at about 1105 cm⁻¹ may be ascribed to Ti-O-C, indicating a slight connection effect between CNT and Ti-O bonds [27]. It means that the TiO₂ nano-particles are attached chemically to the CNT surfaces and are not easily separated.

SEM Morphology

SEM micrographs of the surface morphology for the NaAlg 100%, NaAlg 97.5%/CNT/TiO₂ 2.5%, NaAlg 95%/CNT/TiO₂ 5%, and NaAlg 90%/CNT/TiO₂ 10% composites are shown in

the Fig. (2:a,b,c,d) respectively. Depending on the amount of CNT/TiO₂ present in the polymer matrix, the morphology of NaAlg-CNT/TiO₂ composite membranes will vary and greatly influence its properties. These images show many aggregates or chunks distributed on the top surface indicating that the CNT/TiO₂ particles tend to form aggregates and dispersed into NaAlg polymer matrix. From the images of pure NaAlg and NaAlg-CNT/TiO₂ composites, it was observed that the apparent roughness and whiteness (due to small particle size) increases with increase of the content of CNT/TiO₂ and its dispersion in polymer matrix. In case of the distribution of grains, the homogeneous grains were seen. But these were accommodated like clusters of grains at different spots of the polymer films. Particularly, the shape of grains almost seemed to be like stones [28]. Nanocomposite showed new interwoven structure acting as conductive pathway and leading to high conductivity as compared to that of pure NaAlg [29].

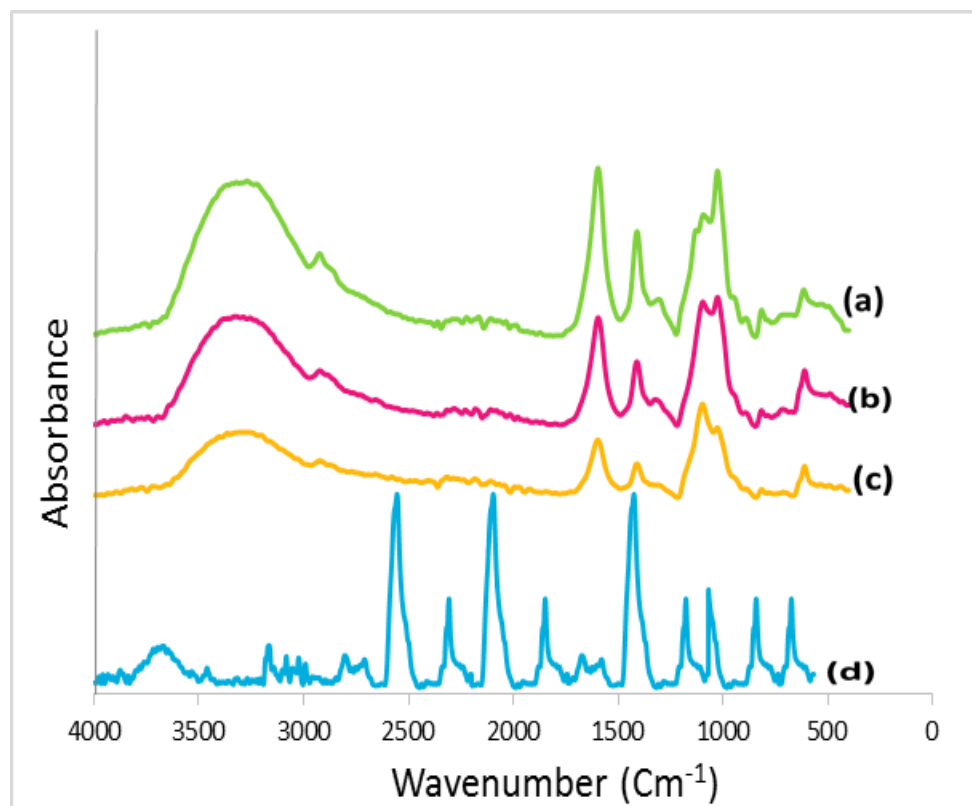


Fig. 1. FTIR Spectra for (a) pure NaAlg, (b) NaAlg-2.5% CNT/TiO₂, (c) NaAlg-5% CNT/TiO₂, (d) NaAlg-10% CNT/TiO₂.

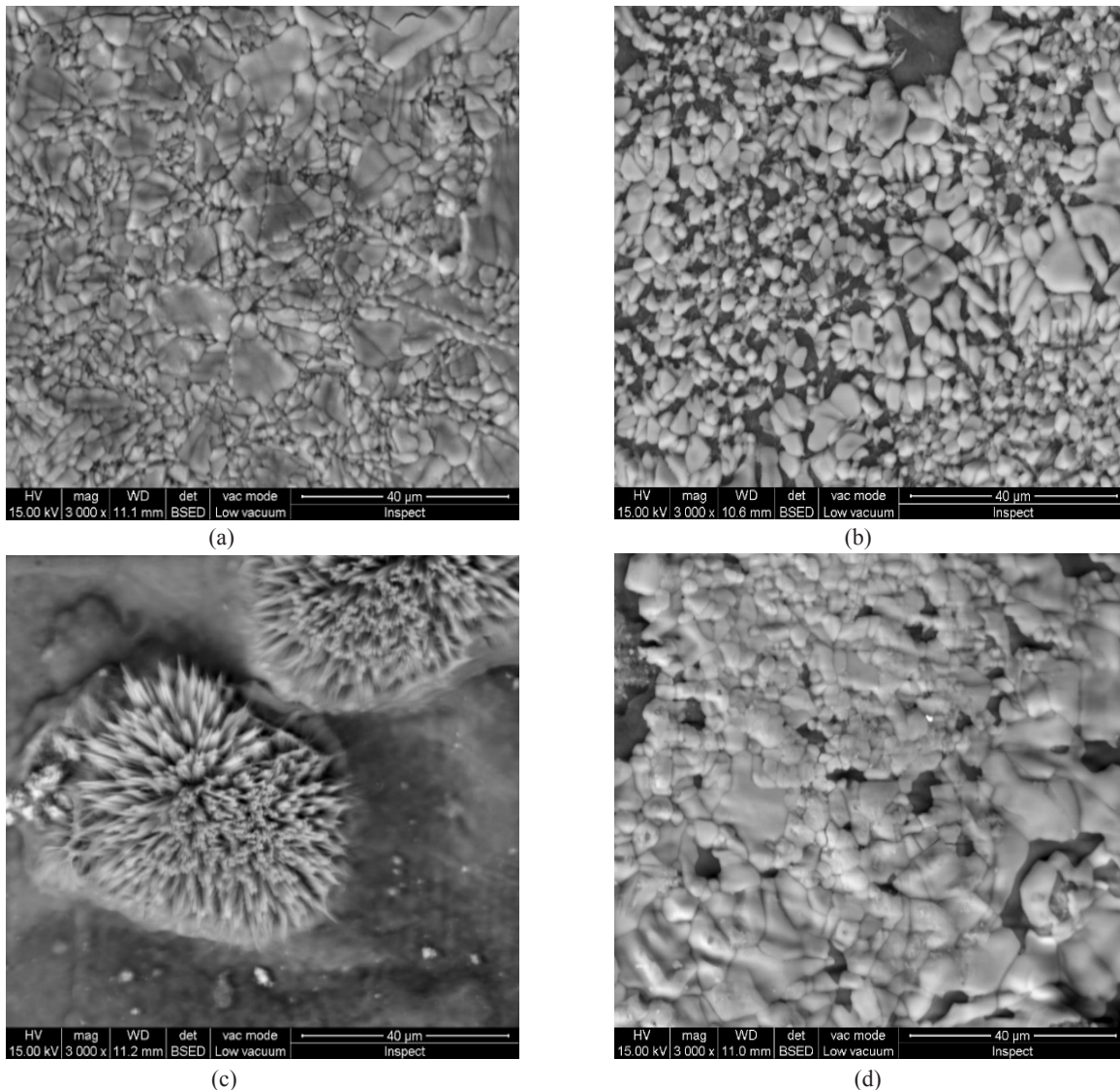


Fig. 2. Scanning electron micrographs for (a) NaAlg (b)(NaAlg) 97.5%/(CNT/TiO₂)2.5%, (c) (NaAlg)95%/(CNT/TiO₂)5%, and (d) (NaAlg) 90%/(CNT/TiO₂) 10%.

Electrical Conductivity Dielectric properties

Temperature and Frequency dependence of (ϵ')

The variation of real part of dielectric constant (ϵ') for NaAlg 100%, NaAlg 97.5%/CNT-TiO₂ 2.5%, NaAlg 95%/CNT/TiO₂ 5%, and NaAlg 90%/CNT/TiO₂ 10% composites as a function of frequency range (42 Hz-1 MHz), and measured at different temperature 308-398°K are shown in Fig. (3:a,b,c,d). It is clear that the dielectric constant increased with increasing temperature. This increase may be attributed to the orientation of the dipoles which are formed from the charge

carriers. The increase in temperature increases the ability of dipoles to align along the applied fields and hence increase the dielectric constant [30]. Also, it can be seen that the dielectric constant of the composites is high at low frequencies and low at higher frequencies. This may be due to the following reason: At higher frequencies of applied signal, response may be given by lesser number of dipole sites as their relaxation time compared to the time required for them to respond to signal, however, at low frequencies, all the available dipole sites respond to the applied signal producing a higher dielectric constant in the sample [30].

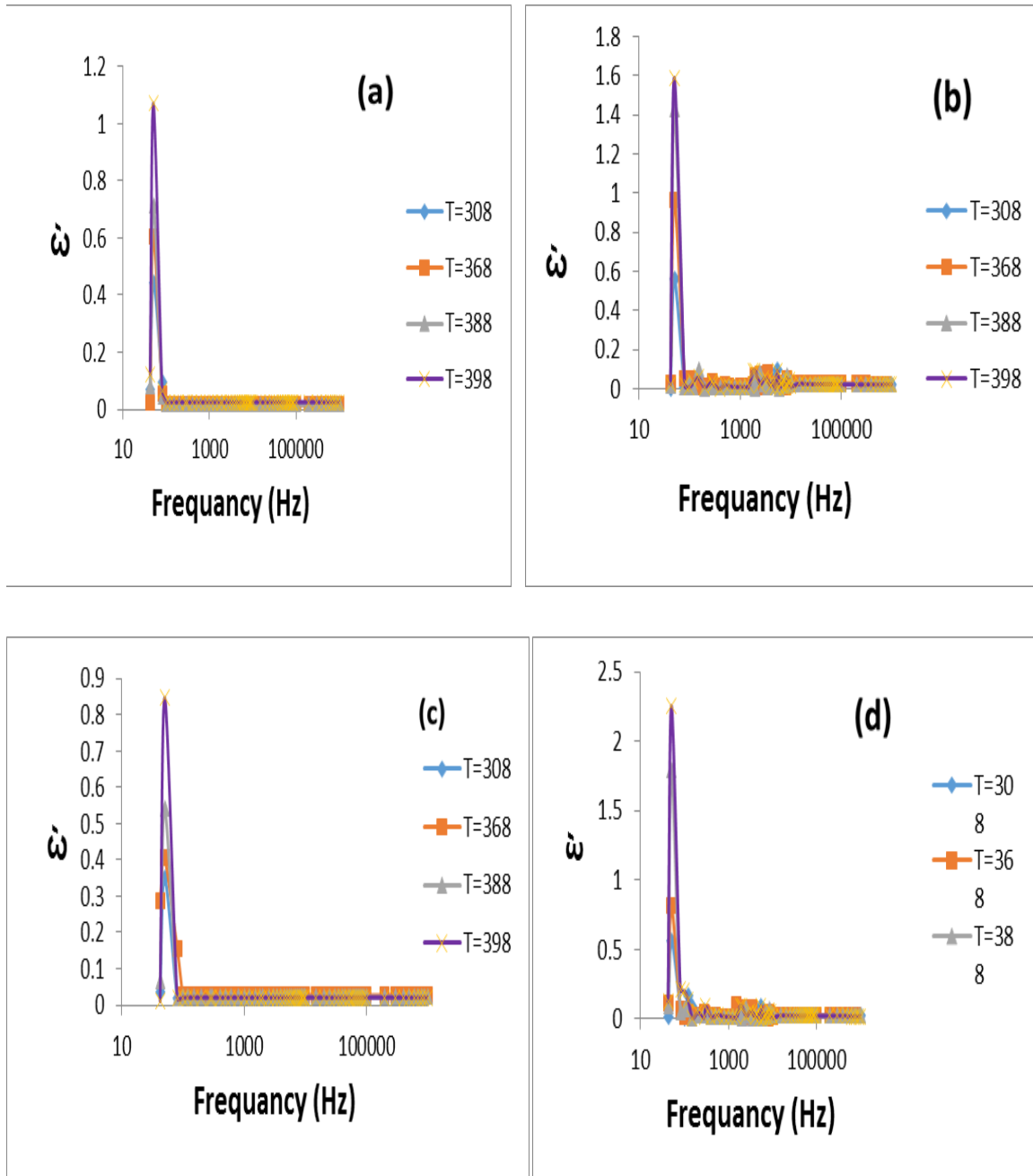


Fig. 3. Frequency and Temperature dependence of ($\dot{\omega}$) for (a) NaAlg (b) NaAlg 97.5%/CNT/TiO₂ 2.5%, (c) NaAlg 95%/CNT/TiO₂ 5%, and (d) NaAlg 90%/CNT/TiO₂ 10%

Temperature and Frequency dependence of ($\dot{\omega}$)

The variation of dielectric loss ($\dot{\omega}$) for NaAlg pure 100%, NaAlg 97.5%/CNT/TiO₂ 2.5%, NaAlg 95%/CNT/TiO₂ 5%, and NaAlg 90%/CNT/TiO₂ 10% composite as a function of frequency range 42 Hz-1 MHz, and measured at different temperature 308-398°K are shown in Fig. (4:a,b,c,d). They exhibit high value of dielectric

loss at low frequencies which can be attributed to the grain boundary effect, since the grain boundaries are more active at lower frequencies. Further at high frequencies, the grains become more active and subsequently, the $\dot{\omega}$ parameter will be reduced. It can be attributed to noticeable enhancement of polarization of composites [31].

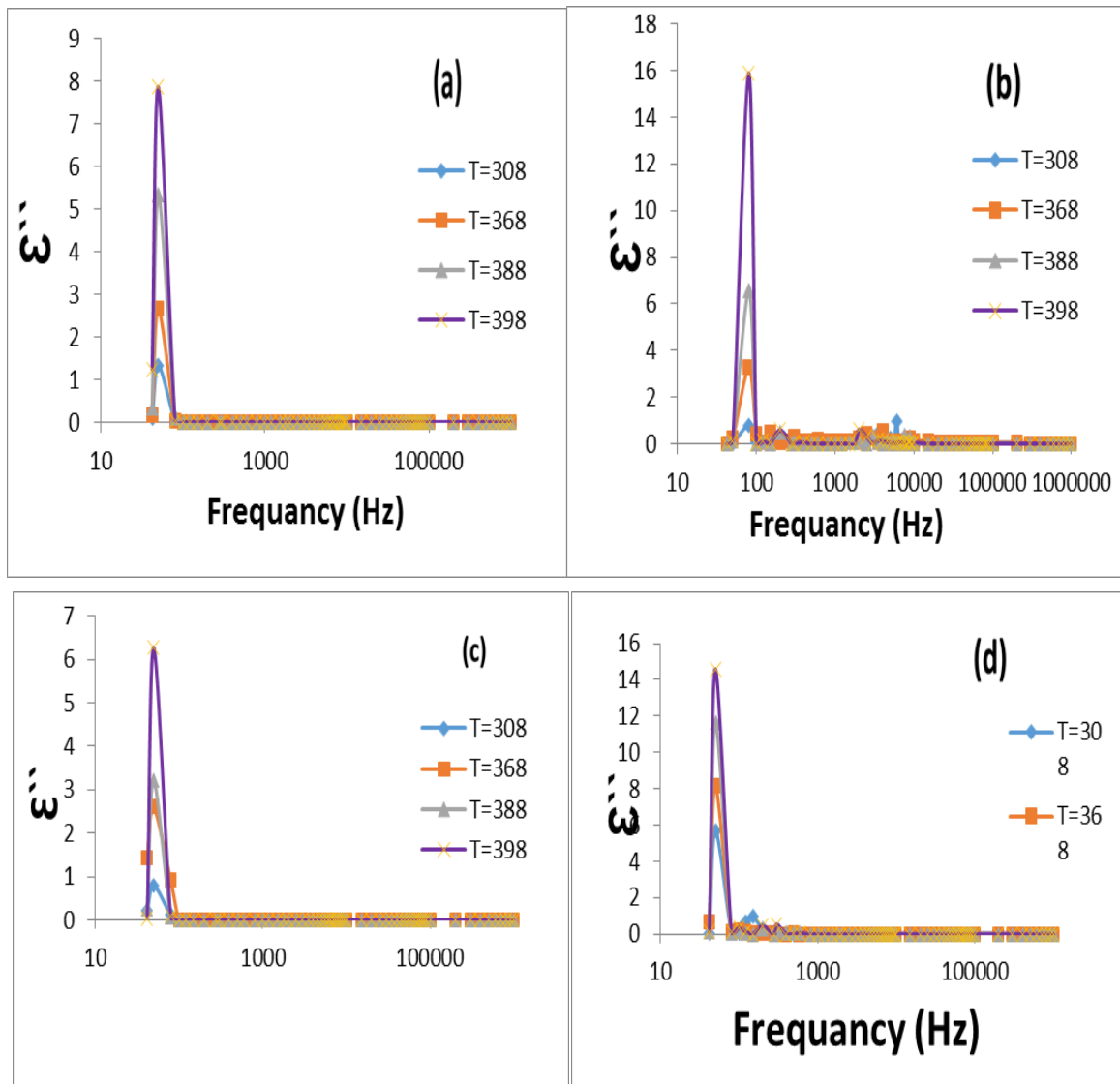


Fig. 4. Frequency and Temperature dependence of $\langle \rangle$ for (a) NaAlg (b) NaAlg 97.5%/CNT/TiO₂ 2.5%, (c) NaAlg 95%/CNT/TiO₂ 5%, and (d) NaAlg 90%/CNT/TiO₂ 10%

Temperature dependence of AC conductivity

Fig. 5 shows the variation of AC conductivity as a function of temperature ranging from 308–398 K for NaAlg pure 100%, NaAlg 97.5%/CNT/TiO₂ 2.5%, NaAlg 95%/CNT/TiO₂ 5%, and NaAlg 90%/CNT/TiO₂ 10%. As the temperature increases, the AC conductivity gradually increases. When CNT/TiO₂ was added into the polymer, it formed a donor-acceptor complex in the conjugated system. As a result, quasi-particles were created apparently polarons (cation) and acted as charge carriers. At low dopant concentration, the polarons have low mobility and exhibit low conductivity. When the polymerization proceeds with increased doping level, more CNT/TiO₂ is

bound to carboxyl group of NaAlg. At this point, many polarons are created and become crowded to have enough energy to form bipolarons (dication). This increases the mobility of the charge carriers which causes the increase in conductivity [32]. Plots of Log (σ) as functions of 1000/T are shown in Fig. 6. This type of electric conductivity behavior follows Arrhenius model [33] and according to this model conductivity-temperature relations $\sigma = \sigma_0 \exp(-E_a/KT)$, where σ_0 is the pre-exponential constant, E_a is the activation energy in eV, K is the Boltzmann's constant, T is the absolute temperature. Activation energy (E_a) is calculated from slope of this plot. The obtained activation energies are also given in table (1).

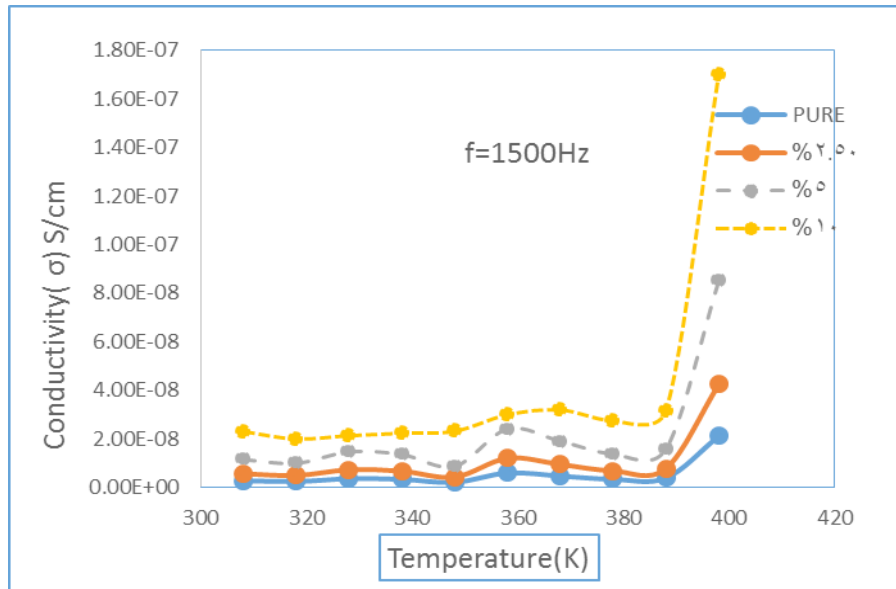


Fig. 5. Plots of conductivity (σ) as a function of Temperatures ranging from 308-398°K at $f=1500$ Hz for (a) NaAlg, (b) NaAlg 97.5%/CNT/TiO₂ 2.5%, (c) NaAlg 95%/CNT/TiO₂ 5%, and (d) NaAlg 90%/CNT/TiO₂ 10% .

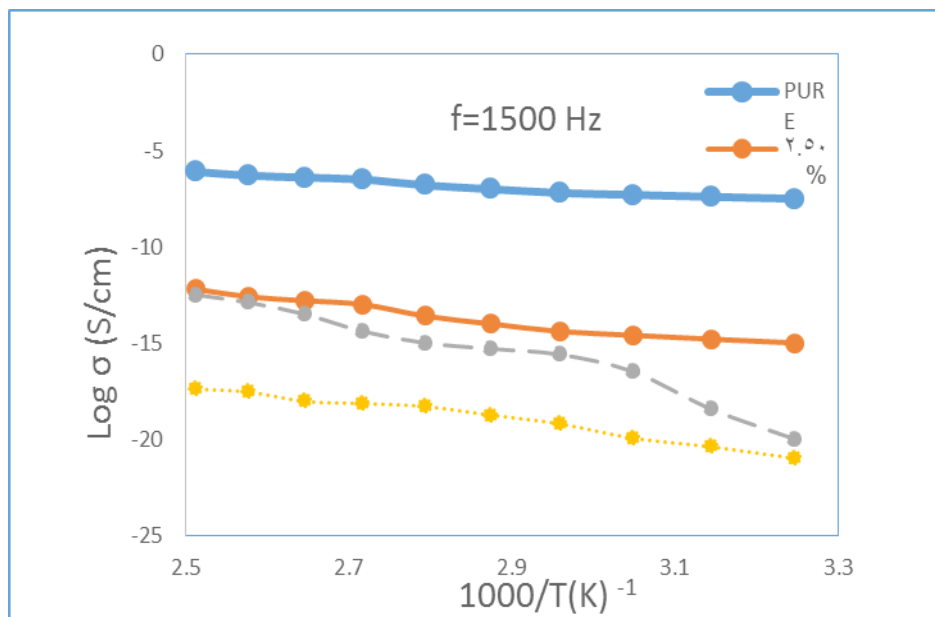


Fig. 6. Plots of Log (σ) as a function of $1000/T$ at $f=1500$ Hz for (a), NaAlg (b) NaAlg 97.5%/CNT/TiO₂ 2.5%, (c) NaAlg 95%/CNT/TiO₂ 5%, and (d) NaAlg 90%/CNT/TiO₂ 10%

TABLE 1. Activation energy for (a) NaAlg, (b) NaAlg 97.5%/CNT/TiO₂ 2.5%, (c) NaAlg 95%/CNT/TiO₂ 5%, and (d) NaAlg 90%/CNT/TiO₂ 10%

Sample	Pure NaAlg	2.5% CNT/TiO ₂	5% CNT/TiO ₂	10% CNT/TiO ₂
Activation Energy(ev)	0.3	0.29	0.28	0.26

Conclusion

NaAlg was successfully treated with TiO₂/CNTs. The morphology of composites was investigated by SEM showing the CNTs coated with NaAlg and TiO₂ dispersed in the alginate matrix. FTIR was applied for characterization of NaAlg composite with TiO₂/CNTs. Comparing with the spectrum of NaAlg beads and NaAlg treated with TiO₂/CNTs, the strong band of NaAlg beads at 1603 cm⁻¹ which is assigned to the carboxyl group shifted from 1608 cm⁻¹ to 1627 cm⁻¹ respectively indicating the specified intermolecular hydrogen bonds between the carboxyl group of NaAlg and TiO₂/CNT. Electrical Conductivity was measured in the range 42 Hz-1 MHz, the study shows that the introduction of TiO₂/CNT results in improvement in electrical conductivity of the NaAlg matrix.

Acknowledgement

The authors would like to thank Prof. Medhat A.A. Ibrahim, at Spectroscopy Department, National Research Centre, and Prof. Hanan Elhaes at Physics Department, Faculty of Women, Ain Shams University for cooperation and facilitating the measurements.

References

1. Ngomsik A.F., Bee A., Siaugue J.M., Talbot D., Cabuil V., Cote G.; Co(II) removal by magnetic alginate beads containing Cyanex 272, *J. Hazard. Mater.*, **166**(2-3), 1043-1049 (2009).
2. Qu J.; Research progress of novel adsorption processes in water purification: A review, *J. Environ. Sci.*, **20**, 1-13 (2008).
3. Trivunac K., Stevanovic S.; Effects of operating parameters on efficiency of cadmium and zinc removal by the complexation-filtration process, *Desalination*, **198**(1-3), 282-287 (2006).
4. Jeon S., Yun J., Lee Y-S., Kim H-I.;
5. Removal of Cu(II) ions by Alginate/Carbon Nanotube/Maghemit Composite Magnetic Beads, *Carbon Lett.*, **11**(2), 117-121 (2010).
6. Md. Shahidul Islam, Md. Ashaduzzaman, Shah Md. Masum, Yeum J.H.; Mechanical and Electrical Properties: Electrospun Alginate/Carbon Nanotube Composite Nanofiber, Dhaka University Journal of Science, **60**(1), 125-128 (2012).
7. Li Y.H., Zhu Y.Q., Zhao Y.M., Wu D.H., Luan Z.K.; Different morphologies of carbon nanotubes effect on the lead removal from aqueous solution, *Diam. Relat. Mater.*, **15**(1), 90-94 (2006).
8. Simon-Deckers A., Gouget B., Mayne-L'Hermite M., Herlin-Boime N., Reynaud C., Carrière M., *Toxicology* **253**(1-3), 137-46 (2008).
9. Hyung H., Fortner J.D., Hughes J.B., Kim J.H.; Natural Organic Matter Stabilizes Carbon Nanotubes in the Aqueous Phase, *Environ. Sci. Technol.*, **41**(1), 179-184 (2007).
10. Li Y., Liu F., Xia B., Du Q., Zhang P., Wang D., Wang Z., Xia Y.J.; Removal of copper from aqueous solution by carbon nanotube/calcium alginate composites, *J. Hazard. Mater.*, **177**(1-3), 876-880 (2010).
11. Zhang J., Xu Q., Feng Z., Li M., Li C.; Importance of the relationship between surface phases and photocatalytic activity of TiO₂, *Angew. Chem. Int. Ed.*, **47**, 1766-1769 (2008).
12. Almeida N.A.F., da Silva P.R., Gonçalves GAB, Marques P.A.A.P., Surface modification of natural and synthetic polymeric fibers for TiO₂-based nanocomposites. In: Mittal V (ed) *Surface modification of nanoparticle and natural fiber fillers. Polymer nano-, micro-macrocomposites*, 7th edn. Wiley, Weinheim, pp 191-219 (2015).
13. Wang Z., Yang C., Lin T., Yin H., Chen P., Wan D., Xu F., Huang F., Lin J., Xie X., Jiang M.; H-doped black titania with very high solar absorption and excellent photocatalysis enhanced by localized surface plasmon resonance, *Adv. Funct. Mater.*, **23**, 5444-5450 (2013).
14. Hoang S., Berglund S.P., Hahn N.T., Bard A.J., Mullins C.B.; Enhancing visible light photo-oxidation of water with TiO₂ nanowire arrays via cotreatment with H₂ and NH₃; synergistic effects between Ti₃ and N, *J. Am. Chem. Soc.*, **134**, 3659-3662 (2012).
15. Chen J., Qiu F., Xu W., Cao S., Zhu H.; Recent progress in enhancing photocatalytic efficiency of TiO₂-based materials, *Appl. Catal. A Gen.*, **495**, 131-140 (2015).
16. Athanasekou C.P., Romanos G.E., Katsaros F.K., Kordatos K., Likodimos V., Falaras P.; Very

- efficient composite titania membranes in hybrid ultrafiltration/photocatalysis water treatment processes, *J. Membr. Sci.*, **392**, 192-203 (2012).
17. Visa M., Duta A.; Methyl-orange and cadmium simultaneous removal using fly ash and photo-Fenton systems, *J. Hazard. Mater.*, **244**, 773-779 (2013).
 18. Papageorgiou S.K., Katsaros F.K., Favvas E.P., Romanos G.E., Athanasekou C.P., Beltsios K.G., Tzialla O.I., Falaras P.; Alginate fibers as photocatalyst immobilizing agents applied in hybrid photocatalytic/ultrafiltration water treatment processes, *Water. Res.*, **46**, 1858-1872 (2012).
 19. Lei P., Wang F., Gao X.W., Ding Y.F., Zhang S.M., Zhao J.C., Liu S.R., Yang M.S.; Immobilization of TiO_2 nanoparticles in polymeric substrates by chemical bonding for multi-cycle photodegradation of organic pollutants, *J. Hazard. Mater.*, **227**, 185-194 (2012).
 20. Yao S.H., Li J.Y., Shi Z.L.; Immobilization of TiO_2 nanoparticles on activated carbon fiber and its photodegradation performance for organic pollutants, *Particuology*, **8**, 272-278 (2010).
 21. Zhao K., Feng L., Li Z., Fu Y., Zhang X., Wei J., Wei S.; Preparation, characterization and photocatalytic degradation properties of a TiO_2 /calcium alginate composite film and the recovery of TiO_2 nanoparticles, *The Royal Society of Chemistry Adv.*, **4**, 51321–51329 (2014).
 22. Wan Ngah W.S., Fatinathan S.; Adsorption of $\text{Cu}(\text{II})$ ions in aqueous solution using chitosan beads, chitosan-GLA beads and chitosan-alginate beads, *Chem. Eng. J.*, **143**, 62-72 (2008).
 23. Moreno-Garrido I., Campana O., Lubian L.M., Blasco J.; Calcium alginate immobilized marine microalgae: Experiments on growth and short-term heavy metal accumulation, *Mar. Pollut. Bull.* *4th International Conference on Marine Pollution and Ecotoxicology*, **51**, 823-829 (2005).
 24. Lopes S., Bueno L., Júnior F.de Aguiar, Finkler C.; Preparation and characterization of alginate and gelatin microcapsules containing *Lactobacillus rhamnosus*, *An Acad Bras Cienc* **89**(3), 1601-1613 (2017).
 25. Zeng M., Fang Z., Xu C.; Novel method of preparing microporous membrane by selective dissolution of chitosan/polyethylene glycol blend membrane, *J. Appl. Polym. Sci.*, **91**(5), 2840-2847 (2004).
 26. Kondawar S.B., Deshpande M.D., Agrawal S.P.; Transport Properties of Conductive Polyaniiline Nanocomposites Based on Carbon Nanotubes, *International Journal of Composite Materials*, **2**(3), 32-36 (2012).
 27. Mugundan S., Rajamannan B., Viruthagiri G., Shanmugan N., Gobi R., Praveen P.; Synthesis and characterization of undoped and cobalt-doped TiO_2 nanoparticles via sol-gel technique, *Appl. Nanosci.*, **5**(4), 449–456 (2014).
 28. Eshaghi A., Hayeripour S., Eshaghi A.; Photocatalytic decolorization of reactive red 198 dye by a TiO_2 -activated carbon nano-composite derived from the sol-gel method, *Res. Chem. Intermed.*, **42**(3), 2461–2471 (2016).
 29. Padma G.T., Subba Rao T., Chandra Babu Naidu K.; Preparation, characterization and dielectric properties of sodium alginate/titanium dioxide composite membranes, *SN Applied Sciences*, **1**, 75 (2019).
 30. Hill N.E., Vaughn W.E., Price H., Davis M.; Dielectric Properties and Molecular Behaviour D. Van Nostrand. London (1969).
 31. Kumar T.M.M., Praveen D.; Impedance analysis of Sodium alginate: Graphene oxide composite, *IOP Conf. Ser.: Mater. Sci. Eng.*, **310**(1), 012150 (2018).
 32. Kumar N.S., Suvarna R.P., Naidu K.C.B., Grain and grain boundary conduction mechanism in sol-gel synthesized and microwave heated $\text{Pb}_{0.8-y}\text{La}_y\text{Co}_{0.2}\text{TiO}_3$ ($y = 0.2-0.8$) nanofibers, *Mater. Chem. Phys.*, **223**, 241-248 (2019).
 33. Nerkar D.M., Rajwade M.R., Jaware S.E., Padhye G.G.; Preparation and electrical characterization of free standing PVA-PPy- FeCl_3 composite polymer films, *Arch. Appl. Sci. Res.*, **7**(10), 17-24 (2015).

الخواص الطيفية والكهربائية لمركب الجينات الصوديوم $\text{TiO}_2 / \text{CNT}$

نجاء احمد شاهين وريهام كمال عبد الحميد
قسم الفيزياء كلية البناء جامعة عين شمس - القاهرة - مصر.

يصف هذا العمل إعداد وتوصيف ألجينات الصوديوم (NaAlg) التي تعامل مع ثاني أكسيد التيتانيوم (TiO_2) - الأنابيب النانوية الكربونية (CNT). تم فحص مورفولوجيا المركبات عن طريق مسح المجهر الإلكتروني (SEM) والتي تبين ان CNT يغطي سطح NaAlg بينما TiO_2 ينتشر مصوفة NaAlg. تم تطبيق التحليل الطيفي للأشعة تحت الحمراء (FTIR) لتوصيف مركب Alg مع NaAlg ، عرضت الجينات بأكملها في منطقة 948-780 سم. تميزت خصائص التركيب وخصائص السطح للعينات بالتوسيع الكهربائي الذي تم قياسه في حدود (MHz- 42 Hz 1). وخلصت الدراسة إلى أن إضافة $\text{TiO}_2 / \text{CNT}$ أدى إلى تحسن في التوصيل الكهربائي لمصوفة NaALg.